

Photoinduced Electron and Energy Transfer in Rigidly Bridged Ru(II)–Rh(III) Binuclear Complexes

Maria Teresa Indelli,^{*,†} Franco Scandola,^{*,†} Jean-Paul Collin,^{*,‡} Jean-Pierre Sauvage,^{*,‡} and Angelique Sour[‡]

Centro di Fotoreattività e Catalisi CNR, Dipartimento di Chimica, Università di Ferrara, 44100 Ferrara, Italy, and Laboratoire de Chimie Organo-Minérale, Institut de Chimie, Université L. Pasteur, 67000 Strasbourg, France

Received June 15, 1995[⊗]

A series of binuclear Ru(II)–Rh(III) complexes of general formula (ttpy)Ru-tpy-(ph)_n-tpy-Rh(tppy)⁵⁺ (*n* = 0–2) have been synthesized, where ttpy = 4'-*p*-tolyl-2,2':6,2''-terpyridine and tpy-(ph)_n-tpy represents a bridging ligand where two 2,2':6,2''-terpyridine units are either directly linked together (*n* = 0) or connected through one (*n* = 1) or two (*n* = 2) phenyl spacers in the 4'-position. This series of complexes is characterized by (i) rigid bridge structures and (ii) variable metal–metal distances (11 Å for *n* = 0, 15.5 Å for *n* = 1, 20 Å for *n* = 2). The photophysics of these binuclear complexes has been investigated in 4:1 methanol/ethanol at 77 K (rigid glass) and 150 K (fluid solution) and compared with that of mononuclear [Ru(tppy)₂²⁺ and Rh(tppy)₂³⁺] or binuclear [(ttpy)Ru-tpy-Rh(tppy)⁴⁺] model compounds. At 77 K, no quenching of the Ru(II)-based excited state is observed, whereas energy transfer from excited Rh(III) to Ru(II) is observed for all complexes. At 150 K, energy transfer from excited Rh(III) to Ru(II) is again observed for all complexes, while quenching of excited Ru(II) by electron transfer to Rh(III) is observed, but only in the complex with *n* = 0. The reasons for the observed behavior can be qualitatively understood in terms of standard electron and energy transfer theory. The different behavior between *n* = 0 and *n* = 1, 2 can be rationalized in terms of better electronic factors and smaller reorganizational energies for the former species. The freezing of electron transfer quenching but not of energy transfer, in rigid glasses reflects the different reorganizational energies involved in the two processes. Unusual results arising from multiphotonic and conformational effects have also been observed with these systems.

Introduction

Covalently-linked donor-acceptor systems¹ are a class of supramolecular systems of great photochemical interest. The simplest systems of this type, two-component "dyads", are suited for the study of photoinduced electron and energy transfer processes.^{1–39} From a fundamental standpoint, such unimolecular processes are free from many of the kinetic complications

inherent to bimolecular analogs. Indeed, studies on dyads have greatly contributed to shaping our understanding of the effect

[†] Università di Ferrara.

[‡] Université L. Pasteur.

[⊗] Abstract published in *Advance ACS Abstracts*, December 1, 1995.

- Balzani, V.; Scandola, F. *Supramolecular Photochemistry*; Horwood: Chichester, U.K., 1991; Chapters 5 and 6.
- Joran, A. D.; Leland, B. A.; Felker, P. M.; Zewail, A. H.; Hopfield, J. J.; Dervan, P. B. *Nature* **1987**, *327*, 508.
- Closs, G. L.; Miller, J. R. *Science* **1988**, *240*, 440.
- Closs, G. L.; Johnson, M. D.; Miller, J. R.; Piotrowiak, P. *J. Am. Chem. Soc.* **1989**, *111*, 3751.
- Sigman, M. E.; Closs, G. L. *J. Phys. Chem.* **1991**, *95*, 5012.
- Wasielowski, M. R. In *Photoinduced Electron Transfer*; Fox, M. A., Chanon, M., Eds.; Elsevier: Amsterdam, 1988; Part A, p 161.
- Wasielowski, M. R. *Chem. Rev.* **1992**, *92*, 435.
- Connolly, J. S.; Bolton, J. R. In *Photoinduced Electron Transfer*; Fox, M. A., Chanon, M., Eds.; Elsevier: Amsterdam, 1988; Part D, p 303.
- Finckh, P.; Heitele, H.; Volk, M.; Michel-Beyerle, M. E. *J. Phys. Chem.* **1988**, *92*, 6584.
- Oevering, H.; Verhoeven, J. W.; Paddon-Row, M. N.; Cotsaris, E.; Hush, N. S. *Chem. Phys. Lett.* **1988**, *150*, 179.
- Verhoeven, J. W.; Kroon, J.; Paddon-Row, M. N.; Warman, J. M. In *Supramolecular Chemistry*; Balzani, V., De Cola, L., Eds.; Kluwer: Dordrecht, The Netherlands, 1992; p 181.
- Verhoeven, J. W.; Paddon-Row, M. N.; Warman, J. M. In *Photoprocesses in Transition Metal Complexes, Biosystems and Other Molecules. Experiments and Theory*; Kochanski, E., Ed.; Kluwer: Dordrecht, The Netherlands, 1992.
- Verhoeven, J. W.; Wegewijs, B.; Kroon, J.; Rettschnick, R. P. H.; Paddon-Row, M. N.; Oliver, A. M. *J. Photochem. Photobiol.* **1994**, *82*, 161.
- Scholes, G. D.; Ghiggino, K.; Oliver, A. M.; Paddon-Row, M. N. *J. Phys. Chem.* **1993**, *97*, 11871.

- Tapolsky, G.; Deusing, R.; Meyer, T. J. *J. Phys. Chem.* **1989**, *93*, 3885.
- Loeb, B. L.; Neyhart, G. A.; Worl, L. A.; Danielson, E.; Sullivan, B. P.; Meyer, T. J. *J. Phys. Chem.* **1989**, *93*, 717.
- MacQueen, D. B.; Schanze, K. S. *J. Am. Chem. Soc.* **1991**, *113*, 7470.
- MacQueen, D. B.; Eyley, J. R.; Schanze, K. S. *J. Am. Chem. Soc.* **1992**, *114*, 1897.
- Ryu, C. K.; Wang, R.; Schmehl, R. H.; Ferrere, S.; Ludwikow, M.; Merkert, J. W.; Headford, C. E. L.; Elliott, C. M. *J. Am. Chem. Soc.* **1992**, *114*, 430.
- Chambron, J.-C.; Coudret, C.; Collin, J.-P.; Guillerez, S.; Sauvage, J.-P.; Barigelletti, F.; Balzani, V.; De Cola, L.; Flamigni, L. *Chem. Rev.* **1994**, *94*, 993.
- Barigelletti, F.; Flamigni, L.; Balzani, V.; Collin, J.-P.; Sauvage, J.-P.; Sour, A.; Constable, E. C.; Cargill Thompson, A. M. W. *J. Am. Chem. Soc.* **1994**, *116*, 7692.
- De Cola, L.; Balzani, V.; Barigelletti, F.; Flamigni, L.; Belser, P.; von Zelewsky, A.; Frank, M.; Vogtle, F. *Inorg. Chem.* **1993**, *32*, 5228.
- Vögtle, F.; Frank, M.; Nieger, M.; von Zelewsky, A.; Balzani, V.; Barigelletti, F.; De Cola, L.; Flamigni, L. *Angew. Chem., Int. Ed. Engl.* **1993**, *32*, 1643.
- van Diemen, J. H.; Hage, R.; Hasnoot, J. G.; Lempers, H. E. B.; Reedijk, J.; Vos, J. G.; De Cola, L.; Barigelletti, F.; Balzani, V. *Inorg. Chem.* **1992**, *31*, 3518.
- Hughes, H. P.; Martin, D.; Bell, S.; McGarvey, J. J.; Vos, J. G. *Inorg. Chem.* **1993**, *32*, 4402.
- Furue, M.; Hirata, M.; Kinoshita, S.; Kushida, T.; Kamachi, M. *Chem. Lett.* **1990**, 2065.
- Nozaki, K.; Ohno, T.; Haga, M. *J. Phys. Chem.* **1992**, *96*, 10880.
- Kalyanasundaram, K.; Graetzel, M.; Nazeeruddin, M. K. *J. Phys. Chem.* **1992**, *96*, 5865.
- Song, X.; Lei, Y.; Van Wallendael, S.; Perkovic, M. W.; Jackman, D. C.; Endicott, J. F.; Rillema, D. P. *J. Phys. Chem.* **1993**, *97*, 3225.
- Scandola, F.; Indelli, M. T.; Chiorboli, C.; Bignozzi, C. A. *Top. Curr. Chem.* **1990**, *158*, 73.
- Scandola, F.; Bignozzi, C. A.; Indelli, M. T. In *Photosensitization and Photocatalysis Using Inorganic and Organometallic Compounds*; Kalyanasundaram, K., Grätzel, M., Eds.; Kluwer: Dordrecht, The Netherlands, 1993; p 161.

of basic physical factors (energy gradient, distance, intervening bonds, medium, etc.) on the kinetics of electron and energy transfer processes. On the other hand, very interesting applications of electron and energy transfer in more complex covalently-linked systems can be envisioned.^{40–42} In multicomponent systems such as “triads”, “tetrads”, etc., light absorption can trigger sequences of electron transfer processes which, under appropriate kinetic control, yield vectorial transport of electronic charge.^{43–47} Also, energy transfer can be used, upon appropriate organization in space and energy, to channel the excitation energy from many chromophoric components to a common acceptor component.^{48–52} On this basis, important functions⁴³ such as the *antenna effect* and *photoinduced charge separation* can be obtained with relatively simple systems, and sensible approaches toward more complex supramolecular systems for artificial photosynthesis can be devised.^{43–47}

Inorganic dyads, where the active components are transition metal complexes, are attractive systems from several viewpoints. In particular, these systems look extremely flexible in terms of tailoring the energetics (excited-state energies, ground- and excited-state redox potentials) by appropriate choice of metals and ligands. A number of inorganic dyads have been synthesized and studied in recent years.^{15–39} Among these, the Ru(II)–Rh(III) dyad Ru^{II}(Me₂phen)₂(Mebpy–CH₂CH₂–Mebpy)–Rh^{III}(Me₂bpy)₂⁵⁺ (Me₂phen = 4,7-dimethyl-1,10-phenanthroline; Mebpy = 4-methyl-2-bipyridyl; Me₂bpy = 4,4'-dimethyl-2,2'-bipyridine) was found to display a variety of intercomponent energy and electron transfer processes.³⁹

The subject of the present work is a series of related Ru(II)–Rh(III) dyads, **Ru-Rh**, **Ru-(ph)-Rh**, and **Ru-(ph)₂-Rh**, schematically shown in Figure 1b. The main differences with

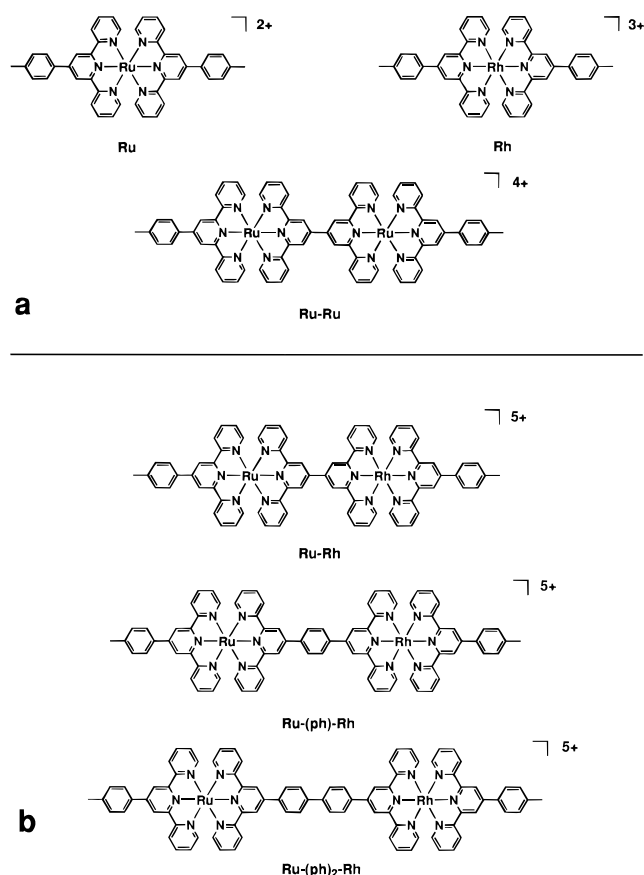


Figure 1. Structural formulas of the Ru(II)–Rh(III) complexes.

respect to the previously studied system³⁹ are (i) the presence of two terdentate ligands (based on 2,2':6',2''-terpyridine, tpy) at each metal center, instead of three bidentate ones, (ii) the rigid nature of the bridges, ensuring a very strict control over the metal–metal distance, and (iii) the tunability of the metal–metal distance by insertion of a variable number of phenyl spacers between the two metal complex fragments. Terpyridine complexes have several structural advantages over analogous bipyridine-based species.²⁰ In this specific case, point ii should minimize kinetic complications³⁹ arising from conformational freedom. Point iii should allow the investigation of the distance dependence of the electron and energy transfer processes, and point i can be of special relevance toward the extension from dyads to triad systems capable of performing two-step photoinduced charge separation (e.g., from Ru(II)–Rh(III) to Ru(II)–Rh(III)–A, where A represents a secondary electron acceptor). With compounds based on tris-bidentate ligands, in fact, this extension would meet with severe problems related to the presence of geometrical isomers at the central unit of the triad. Such problems are absent with complexes of the type shown in Figure 1b, where the trans geometry at each metal center is warranted. Together with these structural advantages, complexes of such type have at least one experimental drawback. In fact, excited Ru(II) bis(terpyridine) complexes are exceedingly weak emitters, with very short (subnanosecond) lifetimes, at room temperature.²⁰ Therefore, low-temperature measurements must be provided for, when such systems are studied.

We report here the photophysical properties of the Ru(II)–Rh(III) binuclear complexes shown in Figure 1b, with particular regard to the possibility of observing intercomponent energy and electron transfer processes. For purposes of comparison, the properties of the mono- and binuclear complexes shown in Figure 1a, suitable as model compounds (see Discussion), are also reported.

- (32) Chiorboli, C.; Bignozzi, C. A.; Indelli, M. T.; Rampi, M. A.; Scandola, F. *Coord. Chem. Rev.* **1991**, *111*, 267.
- (33) Bignozzi, C. A.; Bortolini, O.; Chiorboli, C.; Indelli, M. T.; Rampi, M. A.; Scandola, F. *Inorg. Chem.* **1992**, *31*, 172.
- (34) Indelli, M. T.; Scandola, F. *J. Phys. Chem.* **1993**, *97*, 3328.
- (35) Bignozzi, C. A.; Chiorboli, C.; Indelli, M. T.; Scandola, F.; Bertolasi, V.; Gilli, G. *J. Chem. Soc., Dalton Trans.* **1994**, 2391.
- (36) Bignozzi, C. A.; Argazzi, R.; Schoonover, J. R.; Gordon, K.; Dyer, R. B.; Scandola, F. *Inorg. Chem.* **1992**, *31*, 5260.
- (37) Bignozzi, C. A.; Argazzi, R.; Chiorboli, C.; Scandola, F.; Dyer, R. B.; Schoonover, J. R.; Meyer, T. J. *Inorg. Chem.* **1994**, *33*, 1652.
- (38) Schoonover, J. R.; Gordon, K. C.; Argazzi, R.; Woodruff, W. H.; Peterson, K. A.; Bignozzi, C. A.; Dyer, R. B.; Meyer, T. J. *J. Am. Chem. Soc.* **1993**, *115*, 10996.
- (39) Indelli, M. T.; Bignozzi, C. A.; Harriman, A.; Schoonover, J. R.; Scandola, F. *J. Am. Chem. Soc.* **1994**, *116*, 3768.
- (40) Balzani, V.; Scandola, F. *Supramolecular Photochemistry*, Horwood: Chichester, U. K., 1991; Chapter 12.
- (41) Balzani, V.; Scandola, F. In *Comprehensive Supramolecular Chemistry*; Reinhoudt, D. N., Ed.; Pergamon Press: Oxford, U.K., Vol. 10, in press.
- (42) Balzani, V.; Credi, A.; Scandola, F. In *Transition Metals in Supramolecular Chemistry*; Fabbrizzi, L., Ed.; Kluwer: Dordrecht, The Netherlands, 1994; p 1.
- (43) Gust, D.; Moore, T. A. *Science* **1989**, *244*, 35.
- (44) Gust, D.; Moore, T. A.; Moore, A. L. *Acc. Chem. Res.* **1993**, *26*, 198.
- (45) Larson, S. L.; Cooley, L. F.; Elliott, C. M.; Kelley, D. K. *J. Am. Chem. Soc.* **1992**, *114*, 9504.
- (46) Meckleburg, S. L.; Peek, B. M.; Schoonover, J. R.; McCafferty, D. G.; Wall, C. G.; Erickson, B. W.; Meyer, T. J. *J. Am. Chem. Soc.* **1993**, *115*, 5479.
- (47) Collin, J.-P.; Guillerez, S.; Sauvage, J.-P.; Barigelletti, F.; De Cola, L.; Flamigni, L.; Balzani, V. *Inorg. Chem.* **1992**, *31*, 4112.
- (48) Harriman, A. In *Supramolecular Photochemistry*; Balzani, V., Ed.; Reidel: Dordrecht, 1987; p 207.
- (49) Davila, J.; Harriman, A.; Milgrom, L. R. *Chem. Phys. Lett.* **1987**, *136*, 427.
- (50) Anderson, S.; Anderson, H. L.; Sanders, J. K. M. *Angew. Chem., Int. Ed. Engl.* **1992**, *31*, 907.
- (51) Denti, G.; Campagna, S.; Serroni, S.; Ciano, M.; Balzani, V. *J. Am. Chem. Soc.* **1992**, *114*, 2944.
- (52) Serroni, S.; Denti, G.; Campagna, S.; Juris, A.; Ciano, M.; Balzani, V. *Angew. Chem., Int. Ed. Engl.* **1992**, *31*, 1493.

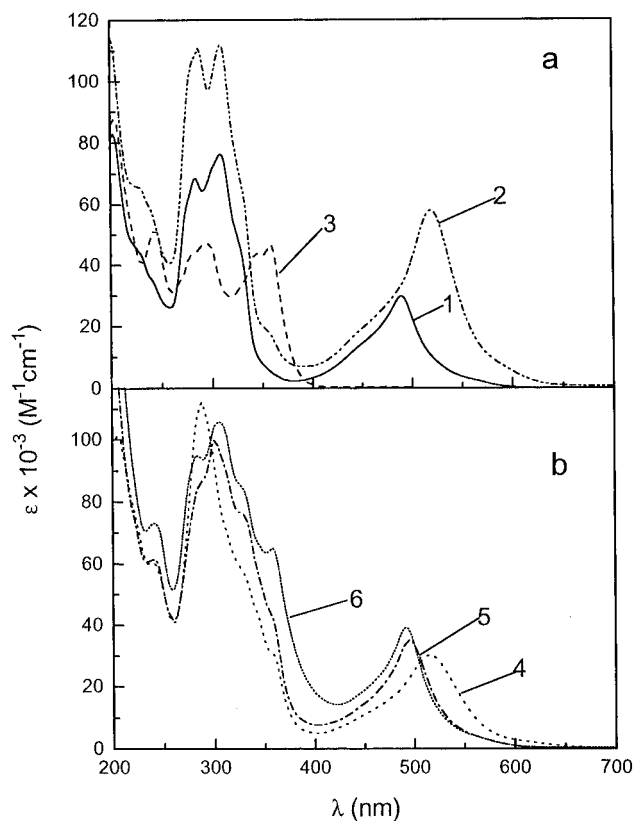


Figure 2. Absorption spectra in acetonitrile solution at room temperature: (a) of the model compounds **Ru** (1), **Ru-Ru** (2), **Rh** (3); (b) of Ru(II)–Rh(III) binuclear complexes **Ru-Rh** (4), **Ru-(ph)-Rh** (5), **Ru-(ph)₂-Rh** (6).

by ligand scrambling. Indeed, the coordination sphere of the rhodium(I) metal is labile and ligand interchange can easily occur. This assumption is confirmed in the synthesis of an asymmetrical bis(terpyridine)rhodium(III) complex. A prolonged reaction of the rhodium precursor Rh(tpy)L₃³⁺ with 4-anisyl-2,2':6',2''-terpyridine (atpy) leads to three complexes Rh(tpy)(atpy)³⁺, Rh(tpy)₂³⁺, and Rh(atpy)₂³⁺ in statistical proportion, respectively 50, 25, and 25% as indicated by ¹H NMR and FAB-MS spectra.

Absorption Spectra. The absorption spectra of the Ru(II)–Rh(III) binuclear complexes are shown in Figure 2 together with the spectra of some model compounds (see Discussion). The visible region is characterized by the metal-to-ligand charge transfer (MLCT) transitions of the Ru(II) component. For **Ru-(ph)-Rh** and **Ru-(ph)₂-Rh**, the MLCT absorption maxima practically coincide with that of the **Ru** model. For **Ru-Rh**, on the other hand, the MLCT absorption maximum is substantially red-shifted with respect to **Ru** and exactly coincides with that of the **Ru-Ru** model. The UV region is dominated by ligand-centered (LC) transitions of both the Ru(II) and Rh(III) components. The comparison with the spectrum of the **Rh** model complex allows us to assign the shoulders at 360 and 330 nm to the Rh(III) component. With increasing number of phenyl groups, the absorption in this spectral region increases and shifts slightly to lower energy.

Electrochemical Behavior. The electrochemical results obtained for the Ru(II)–Rh(III) binuclear complexes are gathered in Table 1 together with the results available for the model complexes. In the binuclear complexes, ruthenium is oxidized at slightly more positive potentials with respect to **Ru**. As the metal–metal separation distance decreases, a gradual anodic shift in the redox potential is observed. For **Ru-Rh**,

Table 1. Redox Potentials of the Ru(II)–Rh(III) Binuclear Complexes and of the Model Compounds^a

complex	redox process			
	Ru(III)/Ru(II)	Rh(III)/Rh(I)	L/L ⁻ (1)	L/L ⁻ (2)
Ru	+1.25		-1.24	-1.46
Ru-Ru ^b	+1.31		-0.93	-1.24
Rh		-0.54 ^c		
Ru-Rh	+1.31	-0.54 ^c	-1.22	-1.44
Ru-(ph)-Rh	+1.29	-0.56 ^c	-1.18	-1.41
Ru-(ph)₂-Rh	+1.27	-0.56 ^c	-1.20	-1.37

^a Cyclic voltammetry in CH₃CN solution at room temperature, 0.1 M Bu₄NBF₄, glassy carbon working electrode, vs SCE; values calculated as averages of the cathodic and anodic peaks. ^b From ref 53. ^c Irreversible process; cathodic peak potential.

the redox potential is substantially more positive with respect to **Ru**. The value for **Ru-Rh** is exactly the same as that for **Ru-Ru**.

As far as reduction is concerned, in the 0.0–1.5 V vs SCE cathodic range, a two-electron irreversible process followed by two reversible reduction waves is observed. The first process is assigned by comparison with the behavior of the **Rh** model to the Rh(III) component. The irreversible character of this reduction process is expected on the basis of what is known about the redox behavior of Rh(III) polypyridine complexes^{57,58} and strongly suggests that the reduction occurs at the metal. The two subsequent reduction waves fall in the same range of potentials as those for the reduction of the ttpy ligands coordinated to Ru(II) center. Given the irreversible character of the first reduction process, however, it is difficult to say whether such processes involve initial or decomposed species.

Emission Measurements. The photophysical behavior of the binuclear complexes was investigated in 4:1 ethanol/methanol at 300 K, at 150 K (fluid solution), and at 77 K (rigid matrix). The experiments carried out consist generally of comparing the emission properties of the Ru(II)–Rh(III) binuclear complexes with those of the appropriate (see Discussion) model compound. In order to avoid precipitation problems at low temperatures, dilute solutions (5 × 10⁻⁵ M) were always used.

(a) **300 K.** All the complexes examined exhibit exceedingly weak emission at room temperature.^{20,21} Under these conditions, even very small amounts of impurities may alter the results and prevent any meaningful analysis.

(b) **150 K Fluid Solution.** At 150 K, **Ru** and the **Ru-Ru** model complex emit, whereas the **Rh** model is practically nonemitting. All the Ru(II)–Rh(III) binuclear complexes were found to exhibit Ru-based emission. As in the case of absorption (Figure 2), for **Ru-(ph)-Rh** and **Ru-(ph)₂-Rh**, the emission maxima (λ = 655 nm and 648 nm, respectively) are close to that of the **Ru** model (λ = 645 nm). For **Ru-Rh**, on the other hand, the emission maximum (λ = 720 nm) is substantially red-shifted with respect to the **Ru** model and is close to that of the **Ru-Ru** model (λ = 708 nm). For **Ru-(ph)-Rh** and **Ru-(ph)₂-Rh**, experiments carried out upon visible MLCT excitation on absorbance-matched solutions gave the same emission intensity as for **Ru** (Figure 3). This result clearly indicates that, for these binuclear complexes, no quenching of the Ru(II)-based excited state takes place at this temperature. For **Ru-Rh**, on the other hand, the comparison between the

(57) Creutz, C.; Keller, A. D.; Schwartz, H. A.; Sutin, N.; Zipp, A. P. In *Mechanistic Aspects of Inorganic Reactions*; Rorabacher, D. B., Endicott, J. F., Eds.; ACS Symposium Series 198; American Chemical Society: Washington, DC, 1982; p 385 and references therein.

(58) Creutz, C.; Keller, A. D.; Sutin, N.; Zipp, A. P. *J. Am. Chem. Soc.* **1982**, *104*, 3618.

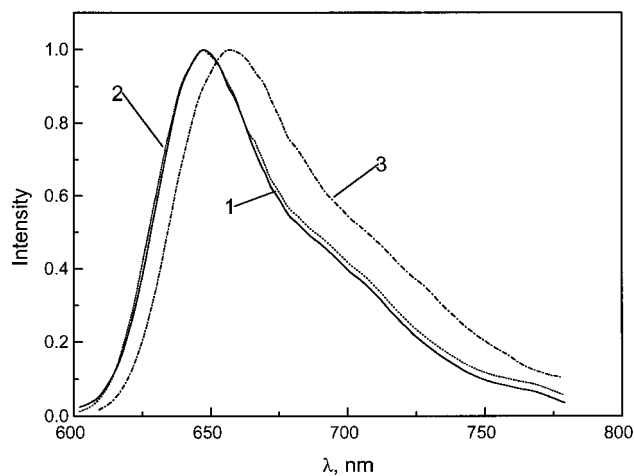


Figure 3. 150 K emission spectra (isoabsorptive solutions, λ_{exc} 490 nm) of **Ru** (1), **Ru-(ph)₂-Rh** (2), and **Ru-(ph)-Rh** (3) in 4:1 ethanol/methanol.

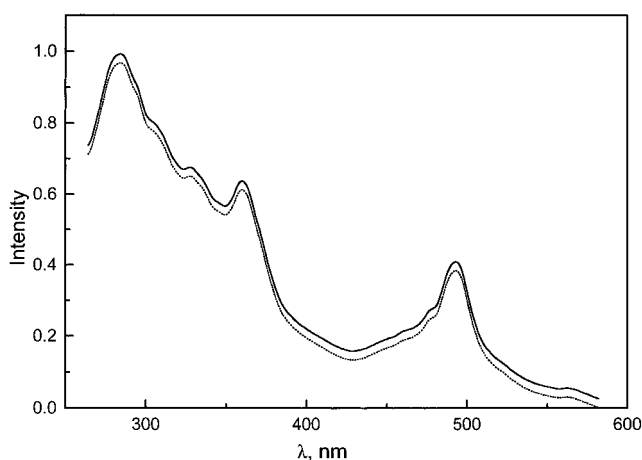


Figure 4. Excitation spectra of **Ru-(ph)₂-Rh** at 150 K (continuous line) and at 77 K (dotted line) in 4:1 ethanol/methanol.

emission quantum yield (Φ) and that of the **Ru-Ru** model (Φ_0) (absorbance-matched solutions at 516 nm excitation wavelength) gave $\Phi_0/\Phi = 5$. This indicates that an efficient quenching of the Ru(II)-based excited state occurs in this complex.

The excitation spectra of the Ru(II)-based emission for **Ru-(ph)₂-Rh** and **Ru-(ph)-Rh** matched very closely the absorption spectra. As an example, the excitation spectrum of **Ru-(ph)₂-Rh** is shown in Figure 4. It can be pointed out that, in this spectrum, features characteristic of the Rh(III) absorption (peaks at 330 and 360 nm) are clearly observed. For **Ru-Rh**, the residual Ru-based emission, much less intense because of the quenching process, was not sufficient to give a precise excitation spectrum.

The emission properties of the binuclear complexes were also studied in pulsed experiments with a Nd/YAG laser at 532 nm. These experiments were initially performed at full laser power, corresponding to 2×10^{-4} M incident photons/pulse. Under these conditions, transient emissions shown in Figure 5 were obtained for **Ru-(ph)₂-Rh** or the **Ru** model. The initial intensity of the transient emission is strongly reduced with respect to the **Ru** model, but the lifetimes are quite comparable (Table 2). There is an evident discrepancy between the apparent quenching (albeit of intensity and not of lifetime) observed in this pulsed experiment and the lack of quenching obtained in the corresponding stationary measurements (Figure 3). In order to explain this discrepancy, laser experiments at varying pulse intensity were performed. At each pulse intensity, the results were qualitatively of the same type as in Figure 5. Upon

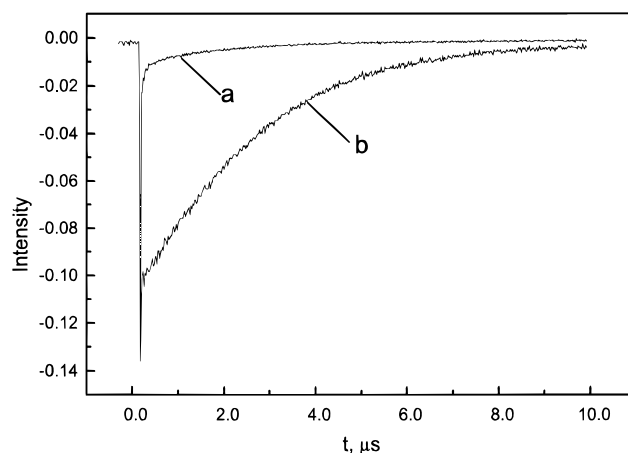


Figure 5. Experimental emission decays recorded at 650 nm following excitation of **Ru-(ph)₂-Rh** (a) and **Ru** (b) at 532 nm (isoabsorptive solutions) with a high intensity (2×10^{-4} M incident photon/pulse) laser pulse.

Table 2. Emission Lifetimes of the Ru(II)–Rh(III) Binuclear Complexes and of the Model Compounds^a

complex	τ (77 K) (μ s)	τ (150 K) ^b (μ s)	complex	τ (77 K) (μ s)	τ (150 K) ^b (μ s)
Ru	13.5	3.2	Ru-Rh	12.5	<0.1
Ru-Ru	12.9	3.5	Ru-(ph)-Rh	13.0	3.0
Rh	2.5	<0.030	Ru-(ph)₂-Rh	13.2	3.5

^a In 4:1 ethanol/methanol. ^b Aerated solution.

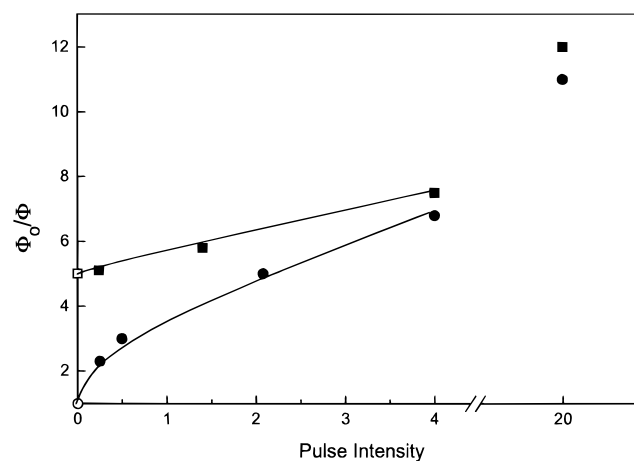


Figure 6. Dependence of the apparent quenching observed in laser experiments (see text) for **Ru-(ph)₂-Rh** (solid circles) and **Ru-Rh** (solid squares) as a function of laser intensity. The open symbols correspond to the Φ_0/Φ values obtained in the stationary spectrofluorimetric experiments. Units of pulse intensity correspond to a concentration of incident photons of 1×10^{-5} M.

decreasing the pulse intensity, however, we observed the difference in intensity between the **Ru-(ph)₂-Rh** and **Ru** traces to decrease. The ratio of emission quantum yields of **Ru** (Φ_0) and **Ru-(ph)₂-Rh** (Φ), obtained from initial intensities and lifetimes of the transient emissions, are plotted as a function of pulse intensity in Figure 6. It is seen that, when the pulse intensity tends to zero, the value of Φ_0/Φ tends to coincide with the result ($\Phi_0/\Phi = 1$) obtained in stationary spectrofluorimetric experiments. In other words, *no quenching takes place at low laser pulse intensity*.

The same type of behavior was observed for the **Ru-(ph)-Ru** complex.

For the **Ru-Rh** complex, qualitatively similar results were also obtained in laser experiments: (i) apparent quenching of emission intensity that decreases with decreasing laser pulse

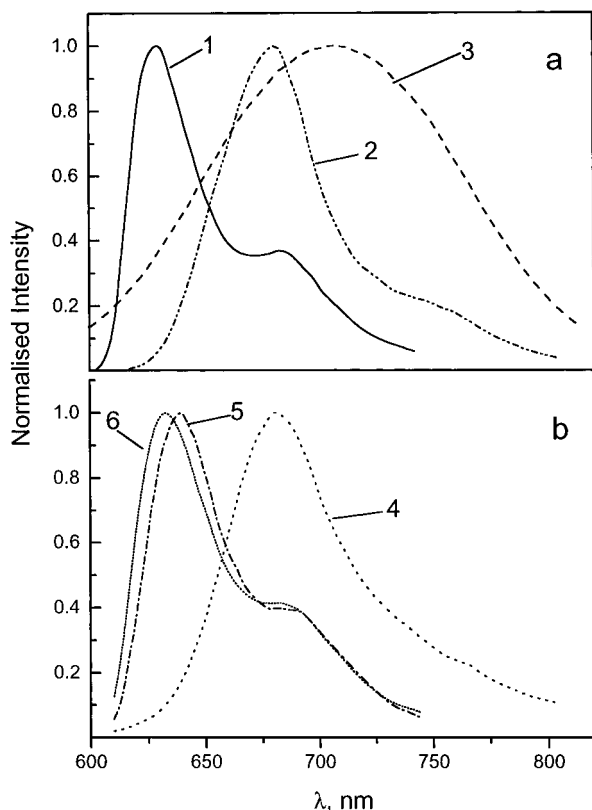


Figure 7. 77 K emission spectra in a 4:1 ethanol/methanol rigid matrix: (a) of the model compounds **Ru** (1), **Ru-Ru** (2), **Rh** (3); (b) of Ru(II)–Rh(III) binuclear complexes (λ_{exc} , 514 nm) **Ru-Rh** (4), **Ru-(ph)-Rh** (5), **Ru-(ph)₂-Rh** (6).

intensity; (ii) residual emission with a long lifetime comparable to that of the **Ru-Ru** model complex. However, for this **Ru-Rh** complex, when the laser intensity tends to zero, the quenching does not disappear completely, but Φ_0/Φ tends to the value ($\Phi_0/\Phi = 5$) obtained in the spectrofluorimetric experiments (Figure 6). No short component experimentally distinguishable from the profile of the excitation pulse ($\tau < 100$ ns) was obtained from the analysis of the emission decay traces measured at any laser intensity.

(c) 77 K Rigid Matrix. As in the 150 K experiments, all the binuclear complexes were found to exhibit Ru-based emission upon visible excitation. There was no indication of any Rh(III)-based emission upon UV excitation. The emission spectra of the binuclear Ru(II)–Rh(III) complexes are shown in Figure 7 together with those of the model compounds. In going from fluid solution to rigid matrix, there is a blue shift, as expected from the MLCT character of the emission.⁵⁹ For **Ru-(ph)₂-Rh** and **Ru-(ph)-Rh**, the emission intensities of absorbance-matched solutions were very close (within the experimental error) to that of the **Ru** model. Also, the emission quantum yield of **Ru-Rh** was practically identical to that of the **Ru-Ru** model. These results clearly indicate that for all complexes no quenching of the Ru-based excited state takes place under these conditions.

In the case of **Ru-Rh**, an anomalous emission behavior was observed. The emission spectrum was remarkably dependent on excitation wavelength (Figure 8a). A corresponding dependence of the maximum of excitation spectrum on the emission wavelength was observed (Figure 8b). A similar anomalous emission behavior was also exhibited by the **Ru-Ru** model.⁶⁰

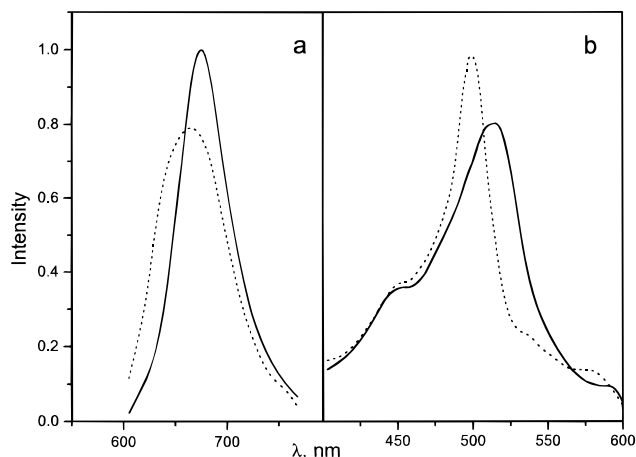


Figure 8. Emission behavior of the **Ru-Rh** complex in 4:1 ethanol/methanol at 77 K: (a) emission spectra obtained upon excitation at 510 nm (continuous line) and at 490 nm (dotted line); (b) excitation spectra measured at λ_{em} 700 nm (continuous line) and at λ_{em} 640 nm (dotted line).

As far as the laser pulsed experiments are concerned, results similar to those observed at 150 K (apparent quenching dependent on laser pulse intensity) were observed, although detailed quantitative experiments were not performed at this temperature. In all cases, the emission decays were strictly exponential with lifetimes practically identical to those of the models (Table 2).

The excitation spectra matched very closely the absorption spectra for all Ru(II)–Rh(III) binuclear complexes. The 77 K excitation spectrum of **Ru-(ph)₂-Rh** is reported in Figure 4, as an example.

Discussion

Molecular Components and Model Compounds. The substantial additivity of the spectroscopic and electrochemical properties of the molecular components in the Ru(II)–Rh(III) binuclear complexes investigated in this study (Figure 2 and Table 1) points toward a relatively weak degree of metal–metal electronic coupling and warrants a localized description of these systems.⁶¹ As usual, some caution must be used in the definitions of the molecular components and of the model compounds that are used to infer their intrinsic properties. For **Ru-(ph)-Rh** and **Ru-(ph)₂-Rh**, the redox potentials for oxidation of ruthenium and reduction of rhodium (Table 1) are very close to those of the mononuclear complexes **Ru** and **Rh**. Also, the MLCT absorption maxima in the visible spectra practically coincide with that of the **Ru** model (Figure 2). For **Ru-Rh**, on the other hand, the redox potential for oxidation of ruthenium and especially the MLCT absorption maximum are substantially shifted (to more positive values and to the red, respectively) with respect to **Ru**. Although this could be taken, at first sight, as an indication of strong metal–metal coupling (perturbation of the properties of the Ru(II) center by the electron-withdrawing Rh(III) center), this explanation is ruled out by the fact that exactly the same shifts are observed for **Ru-Ru** (Table 1 and Figure 2) or the analogous Ru–Os complex.²¹ This indicates that the peculiarity of **Ru-Rh** with respect to the other two

(60) In fluid solution at 150 K, wavelength effects on the emission and excitation spectra disappear for **Ru-Ru**. For **Ru-Rh**, on the other hand, accurate emission/excitation experiments are precluded by the quenching process.

(61) Quantitative evidence for the degree of metal–metal electronic coupling in systems with the same bridges comes from intensities of intervalence transfer transitions in analogous Ru(II)–Ru(III) complexes.⁵³

(59) Juris, A.; Balzani, V.; Barigelletti, F.; Campagna, S.; Belser, P.; von Zelewsky, A. *Coord. Chem. Rev.* **1988**, *27*, 4587.

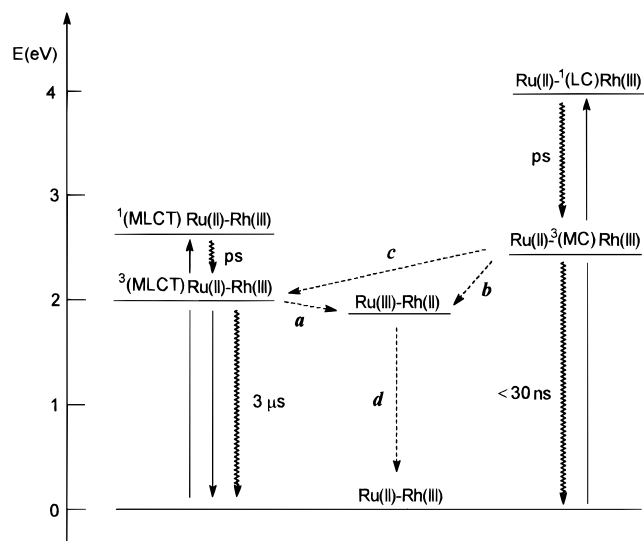


Figure 9. General energy level diagram for the Ru(II)–Rh(III) binuclear complexes. For definition of states, see text. Intracomponent deactivation processes are indicated by continuous arrows. Indicative lifetimes are given for such processes at 150 K. Possible intercomponent transfer processes are indicated by dotted arrows.

members of the series is essentially related to special properties of the “double-terpy” ligand present on the Ru(II) center, quite independent of the nature of the second metal center. Probably because of partial delocalization over the two tpy moieties, this bridging ligand appears to have π^* orbitals of lower energy than the phenylene-linked ones. In conclusion, different compounds should be taken as models for the properties of the molecular components in this series: for the Ru(II) and Rh(III) centers of **Ru-(ph)-Rh** and **Ru-(ph)₂-Rh**, the mononuclear **Ru** and **Rh** complexes provide good models; for the Ru(II) center of **Ru-Rh**, an appropriate model is represented by the binuclear **Ru-Ru** complex.

Energy Levels. A general energy level diagram for the Ru(II)–Rh(III) complexes is shown in Figure 9. The diagram holds for **Ru-Rh**, **Ru-(ph)-Rh**, and **Ru-(ph)₂-Rh**, with minor quantitative differences between the three complexes. The excited states represented are as follows: (i) the local excited states involved in selective excitation of the two molecular components, i.e., the singlet MLCT state of Ru(II) and the singlet ligand-centered (LC) state of Rh(III); (ii) the lowest, long-lived, emitting local excited states, i.e., the triplet MLCT state of Ru(II) and the triplet metal-centered (MC) state of Rh(III);⁶² (iii) the intercomponent electron transfer state. Indicative lifetimes are given, corresponding to the main deactivation processes within each molecular component at 150 K. The values for the lowest triplet excited states are based on direct evidence (Table 2), while the time scale indicated for population of such states from the singlets reached by absorption are based on analogy with what is known for related bipyridine systems.^{63,64} In Figure 9, possible intercomponent transfer processes are indicated by dotted arrows.

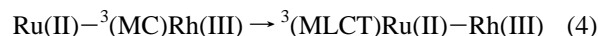
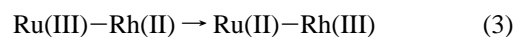
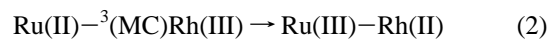
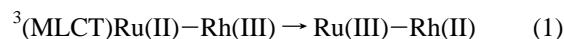
Relevant energy values for the various excited states, obtained from spectroscopic and electrochemical data on complexes and model compounds, are given in Table 3. Two main factors limit the accuracy of the energy estimates in these systems: the

Table 3. Relevant Energy Parameters and Driving Forces for the Intercomponent Processes of Figure 9

complex	E^{0-0} ^a (eV)	$E^{\text{ox}}(\text{Ru}^*)$ ^b (V)	$E^{\text{red}}(\text{Rh}^*)$ ^b (V)	$\Delta G^\circ(a)$ (eV)	$\Delta G^\circ(b)$ (eV)	$\Delta G^\circ(c)$ (eV)
Ru	1.97 ^c	−0.72				
Ru-Ru	1.84 ^c	−0.53				
Rh	2.38 ^d		+1.84			
Ru-Rh	1.84 ^c	−0.53	+1.84	+0.01	−0.53	−0.54
Ru-(ph)-Rh	1.95 ^c	−0.66	+1.82	−0.10	−0.53	−0.43
Ru-(ph)₂-Rh	1.97 ^c	−0.70	+1.82	−0.14	−0.55	−0.41

^a Taken from 77 K emission spectra (Figure 7). ^b Calculated from E^{0-0} and redox potentials of the ground states (Table 1). ^c $\lambda_{\text{em}}^{\text{max}}$. ^d Onset.

irreversible character of the electrochemical Rh(III) reduction and the possibility that the Ru(III)–Rh(II) state is stabilized relative to the electrochemical prediction by intercomponent interaction (the latter effect could be more relevant for the shorter systems, e.g., for **Ru-Rh**, where the slightly positive ΔG° value reported in Table 3 could actually be either zero or even slightly negative). In conclusion, within experimental accuracy, the following predictions can be made concerning the thermodynamic feasibility of the various possible intercomponent transfer processes: (i) energy transfer from excited Rh(III) to Ru(II) (process *c* in Figure 9, eq 4) substantially



exergonic for all complexes; (ii) electron transfer from Ru(II) to excited Rh(III) (process *b* in Figure 9, eq 2) is substantially exergonic for all complexes; (iii) electron transfer from excited Ru(II) to Rh(III) (process *a* in Figure 9, eq 1) is almost isoergonic for **Ru-Rh** and slightly exergonic for **Ru-(ph)-Rh** and **Ru-(ph)₂-Rh**; (iv) charge recombination (process *d* in Figure 9, eq 3) is highly exergonic in all cases.

Photophysics of the Binuclear Complexes. The photophysical behavior of the Ru(II)–Rh(III) systems is complicated by some peculiar effects (conformational problems and multiphotonic effects) which will be discussed in some detail in later sections. Aside from these complications, the main photophysical results can be summarized as follows.

At 77 K, both the stationary spectrofluorimetric results and the pulsed laser results (after cleaning from multiphotonic effects) indicate that the Ru(II)-based excited state is not quenched (relative to the appropriate model compound), for any of the Ru(II)–Rh(III) complexes of this series. This shows that intramolecular electron transfer from excited Ru(II) to Rh(III) (process *a* in Figure 9, eq 1) is inefficient for all complexes under these conditions. Given the lifetime of the Ru(II)-based excited state under these conditions (Table 2), this indicates that the process must have a rate constant $k \leq 10^5 \text{ s}^{-1}$.

At 150 K, both the stationary spectrofluorimetric results and the pulsed laser results of Figure 5 (after consideration of multiphotonic effects, Figure 6) indicate that the Ru(II)-based excited state is substantially (ca. 80%) quenched (relative to the appropriate model compound) for **Ru-Rh** but not for **Ru-(ph)-Rh** and **Ru-(ph)₂-Rh**. This shows that electron transfer from excited Ru(II) to Rh(III) (process *a* in Figure 9, eq 1) is efficient for **Ru-Rh** but not for **Ru-(ph)-Rh** and **Ru-(ph)₂-Rh**. Given the intrinsic lifetimes of the Ru(II)-based excited states of the three complexes in these conditions (Table 2), this means

(62) Frink, M. E.; Sprouse, S. D.; Goodwin, H. A.; Watts, R. J.; Ford, P. C. *Inorg. Chem.* **1988**, *27*, 1283.

(63) Kirk, A. D.; Hoggard, P. E.; Porter, G. B.; Rockley, M. G.; Windsor, M. W. *Chem. Phys. Lett.* **1976**, *37*, 199.

(64) In picosecond laser flash photolysis, formation of the LC triplet state of Rh(III) polypyridine complexes is complete in $\tau < 30 \text{ ps}$ (M. T. Indelli and N. Serpone, unpublished results).

that the process has a rate constant $k \geq 3 \times 10^5 \text{ s}^{-1}$ for **Ru-Rh**⁶⁵ and $k \leq 3 \times 10^5 \text{ s}^{-1}$ for **Ru-(ph)-Rh** and **Ru-(ph)₂-Rh**.

At both 77 and 150 K, the excitation spectra of the Ru(II)-based emission (Figure 4) clearly indicate efficient population of the Ru(II)-based excited state following light absorption by the Rh(III)-based chromophore. This shows that energy transfer from excited Rh(III) to Ru(II) (process *c* in Figure 9, eq 4) is efficient under these conditions. Given the lifetimes of the Rh(III)-based excited state under these conditions (Table 2), this indicates that the process has rate constants $k \geq 4 \times 10^5 \text{ s}^{-1}$ (77 K) and $k \geq 3 \times 10^7 \text{ s}^{-1}$ (150 K) for all complexes. This also shows that the energy transfer process is faster, under these conditions, than the potentially competing electron transfer process from Ru(II) to excited Rh(III) (process *b* in Figure 9, eq 2).

Kinetic Aspects. The above summarized photophysical results can be discussed, and at least qualitatively rationalized, in terms of standard electron transfer theory.^{66–69} Let us assume that intercomponent electronic coupling is sufficiently small that the reactions belong to the nonadiabatic regime. In a simple approximation in which the solvent modes (average frequency, ν_o) are treated classically ($h\nu_o \ll k_B T$) and the internal vibrations are represented by a single mode of average frequency ν_i , thermally frozen and treated quantum mechanically, the rate constant is given by

$$k_{\text{el}} = (2\pi/h)H_{\text{AB}}^2(\text{FCWD}) \quad (5)$$

where H_{AB} is the electronic coupling matrix element and the Franck–Condon weighted density of states, FCWD, is given by

$$\text{FCWD} = \frac{1}{(4\pi\lambda_o k_B T)^{1/2}} e^{-S} \sum_m \frac{S^m}{m!} \exp\left[-\frac{(\Delta G^\circ + \lambda_o + m h\nu_i)^2}{4\lambda_o k_B T}\right] \quad (6)$$

In this expression, $S = \lambda_i/h\nu_i$ is the electron–phonon coupling strength (representing the degree of distortion in the high-frequency mode accompanying electron transfer), λ_i and λ_o are the inner-sphere and outer-sphere reorganizational energies, and the summation extends over the number of quanta of inner vibrational modes in the product state, m .

Values for the parameters in eqs 5 and 6 can be estimated, for the three complexes of the series, under reasonable assumptions. For the outer-sphere reorganizational energy value, λ_o , values of 6200, 8000, and 8800 cm^{-1} are given by the standard two-sphere dielectric continuum model with intercomponent (metal–metal) distances of 11, 15.5, and 20 Å⁵³ for **Ru-Rh**, **Ru-(ph)-Rh**, and **Ru-(ph)₂-Rh**, respectively,⁷⁰ and representa-

tive radii of 5.1 Å for the two metal polypyridine moieties.^{71,72} An inner-sphere frequency value, ν_i , of 500 cm^{-1} could be appropriate for all complexes. This choice reflects the following assumptions: (i) internal reorganization is negligible in the $(t_{2g})^2/(t_{2g})^6$ Ru(III)/Ru(II) couple; (ii) reduction of the Rh(III) terpyridine complexes takes place at the metal center;⁷³ (iii) internal reorganization can be significant for the $(t_{2g})^6/(t_{2g})^6(e_g^*)^1$ Rh(III)/Rh(II) couple.⁷³ A reasonable estimate of the internal part of the reorganizational energy is a value of $S = 2$ (i.e. $\lambda_i = 1000 \text{ cm}^{-1}$).

Individual values of H_{AB} are clearly needed for the three complexes, involving bridges of different length. The relative magnitude of the electronic matrix elements for the three complexes can be inferred from the intensities of the intervalence transfer bands in the analogous Ru(II)–Ru(III) species investigated by Launay and co-workers.⁵³ These intensities yield values of 380, 240, and 180 cm^{-1} for **Ru-Ru**, **Ru-(ph)-Ru**, and **Ru-(ph)₂-Ru**, respectively. A proportional decrease in electronic factors, which reflects the decreasing coupling ability of the bridging ligands, is likely to be appropriate also for the Ru(II)–Rh(III) series. On the other hand, it must be pointed out that absolute values are expected to be smaller for the Ru(II)–Rh(III) case (where the bridge-mediated orbital overlap is between a πt_{2g} orbital of Ru and a σe_g^* orbital of Rh) than for the Ru(II)–Ru(III) case (where the bridge-mediated orbital overlap is between a πt_{2g} orbital of Ru and a πt_{2g} orbital of Ru).⁷⁴ An appropriate scaling down of the Ru(II)–Ru(III) data, based on spectroscopic data for other π – π vs π – σ systems,^{75–77} yields values of 130, 80, and 60 cm^{-1} for **Ru-Rh**, **Ru-(ph)-Rh**, and **Ru-(ph)₂-Rh**, respectively. The above set of parameters, though by no means unique, is based on plausible assumptions and can be used as a basis for discussing the rate-determining factors in this system.

(a) Electron Transfer from Excited Ru(II) to Rh(III) (Process *a* in Figure 9, Eq 1). Using the above discussed set of values and eqs 5 and 6 at 150 K, the following rate constants for electron transfer from excited Ru(II) to Rh(III) are obtained: **Ru-Rh**, $5 \times 10^6 \text{ s}^{-1}$; **Ru-(ph)-Rh**, $1 \times 10^5 \text{ s}^{-1}$; **Ru-(ph)₂-Rh**, $4 \times 10^4 \text{ s}^{-1}$. Since the lifetime of the Ru(II)-based excited state at this temperature is ca. 3 μs for all model complexes (rate constant for excited-state decay ca. $3.3 \times 10^5 \text{ s}^{-1}$), the occurrence of electron transfer quenching for **Ru-Rh** but not for **Ru-(ph)-Rh** and **Ru-(ph)₂-Rh** can be understood, at least qualitatively, on kinetic grounds. The system with the shortest bridge is favored by both a larger electronic factor and a smaller outer-sphere reorganizational energy, despite its apparently less favorable driving force.

The reason for the general slowness of these processes is the low temperature: all of them are in the Marcus “normal” free energy region and thus are thermally activated. Upon an increase in the temperature from 150 K to, e.g., 300 K, the rate

(65) Under the experimental conditions used, the lack of an observable time-resolved fast decay corresponding to the quenched emission suggests a lower limiting value of $5 \times 10^6 \text{ s}^{-1}$.

(66) Marcus, R. A.; Sutin, N. *Biochim. Biophys. Acta* **1985**, *811*, 265.

(67) Jortner, J. *J. Chem. Phys.* **1976**, *64*, 4860.

(68) Sutin, N. *Prog. Inorg. Chem.* **1983**, *30*, 441.

(69) Miller, J. R.; Beitz, J. V.; Huddleston, R. K. *J. Am. Chem. Soc.* **1984**, *106*, 5057.

(70) As correctly pointed out by a reviewer, various types of distances are actually involved in the electron transfer processes of Figure 9: Ru-based tpy fragment to Rh, for electron transfer from excited Ru(II) to Rh(III) (process *a*); metal-to-metal, for electron transfer from excited Rh(III) to Ru(II) (process *b*) and for back electron transfer (process *d*). Unfortunately, such details cannot be accommodated in a simple two-sphere model, where the use of a center-to-center distance is the only allowed option. For this, in addition to the other approximations made in the calculation, the obtained λ_o values should be regarded as indicative figures.

(71) Following the approach of Brunshwig et al.⁷² in the two-sphere model, each molecular component can be modeled by a “representative sphere”, with an effective radius obtainable from CPK models. For both molecular components of our Ru(II)–Rh(III) dyads (identified as (tpy)M(tpy) fragments), this procedure gives a value of 5.1 Å for the radii of the representative spheres.

(72) Brunshwig, B. S.; Ehrenson, S.; Sutin, N. *J. Phys. Chem.* **1986**, *90*, 3657.

(73) This assumption is in line with the observed irreversibility of the Rh(III) reduction.

(74) Braterman, P. S. *J. Chem. Soc. A* **1966**, 1471.

(75) A 3-fold reduction in H_{AB} is found, e.g., by comparing the intervalence transfer bands of $(\text{CN})_5\text{Fe}^{\text{II}}-\text{CN}-\text{Fe}^{\text{III}}(\text{CN})_5^{6-}$ (t_{2g} to t_{2g})⁷⁶ and $(\text{CN})_5\text{Fe}^{\text{II}}-\text{CN}-\text{Co}^{\text{III}}(\text{CN})_5^{6-}$ (t_{2g} to e_g^*)⁷⁷.

(76) Glauser, R.; Hauser, U.; Heren, F.; Ludi, A.; Roder, P.; Schmidt, E.; Siegenthaler, H.; Wenk, F. *J. Am. Chem. Soc.* **1973**, *95*, 8457.

(77) Vogler, A.; Kunkely, H. *Ber. Bunsen-Ges. Phys. Chem.* **1975**, *79*, 301.

constants are expected to increase, according to eqs 5 and 6 from the microsecond to the nanosecond time scale. Unfortunately, however, the lifetimes of the Ru(II)-based excited states in these complexes are also expected to shorten quite substantially with increasing temperature (for $\text{Ru}(\text{tpy})_2^{2+}$ and **Ru** at 293 K, lifetimes of 250 and 950 ps, respectively, have been reported²¹). Thus, with this class of complexes, the experimental window for studying intercomponent electron transfer from excited Ru(II) to Rh(III) is practically very narrow, being limited to **Ru–Rh** at temperatures close to 150 K.

At 77 K, the lack of observable electron transfer quenching of the Ru(II)-based excited state for all complexes is in line with what is expected to occur for processes which are slightly exergonic in fluid solution upon going to a rigid medium. As a matter of fact, any process with $0 > \Delta G^\circ(\text{fluid solution}) > -\lambda_0$ is expected to become thermodynamically unfavorable when the reorientation of the solvent dipoles is frozen in a glassy medium.

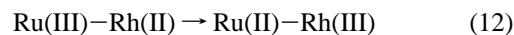
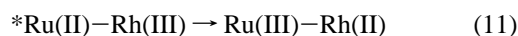
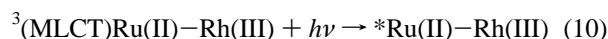
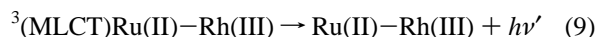
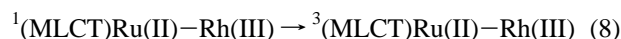
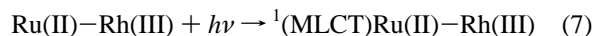
(b) Electron Transfer from Ru(II) to Excited Rh(III) (Process b in Figure 9, Eq 2). The electron transfers from Ru(II) to excited Rh(III), being more exergonic, are expected to be faster than the previously discussed ones, with time scales in the subnanosecond range at 150 K. It is difficult to tell whether such processes could compete with the lifetime of the Rh(III)-based excited state, which is unknown at this temperature but is presumably also in the same range. Experimentally, other processes dominate the photophysics following Rh(III) excitation (see below).

(c) Energy Transfer from Excited Rh(III) to Ru(II) (Process c in Figure 9, Eq 4). Energy transfer from excited Rh(III) to Ru(II), which efficiently takes place following Rh(III) excitation, is clearly fast enough to compete with the presumably very short Rh(III) excited-state lifetime. The reasons can likely be traced back, using formally similar kinetic models for energy^{78,79} and electron transfer, to the much smaller outer-sphere reorganizational energy involved in energy transfer (where, except for the transient dipole moment change associated with the MLCT state at the Ru(II) center, no charges are displaced) relative to electron transfer (where a full electron charge is displaced between the two metal centers). It is thus quite possible that the energy transfer processes in these systems, which are exergonic by ca. 0.5 eV, lie close to the activationless regime. The fact that energy transfer from excited Rh(III) to Ru(II) remains efficient in rigid glasses at 77 K tends to support this view.⁸⁰

(d) Charge Recombination (Process d in Figure 9, Eq 3). Experimental access to this process is precluded by kinetic factors. In fact, this highly exergonic process is expected to take place on the subnanosecond time scale and, lying in the Marcus “inverted” region ($\Delta G^\circ < -\lambda_0$), should be practically independent of temperature.^{66–68} Thus, even in the case where electron transfer from excited Ru(II) to Rh(III) (eq 1) takes place, i.e., for **Ru–Rh** at 150 K, the Ru(III)–Rh(II) state cannot accumulate to any appreciable extent.

Multiphotonic Effects. One of the problems encountered in this study has been an apparent quenching of emission intensity observed in laser experiments, which did not match the spectrofluorimetric results (Figures 3 and 5). The careful examination of the dependence on laser pulse intensity permitted us to establish the multiphotonic origin of such effects. The experimental conclusion is that, in the binuclear Ru(II)–Rh(III) complexes, population of upper excited states of the Ru(II)-based molecular component by multiphoton absorption is followed by some deactivation process leading back to the ground state *without passing through the luminescent MLCT state*. The interesting point here is that no such effects are observed with any of the Ru(II) model compounds, where multiphotonic excitation is apparently followed by deactivation to the luminescent MLCT state. Thus, the nonemissive channel available to the upper Ru(II)-based excited states of the binuclear complexes must involve in some way the rhodium center. Deactivation through Rh(III)-based excited states can be ruled out, as back energy transfer to the emissive Ru(II) MLCT state is known to be efficient in all the systems.

The most plausible hypothesis is that the nonemissive channel goes through the Ru(III)–Rh(II) electron transfer state (eqs 7–12, where *Ru(II)–Rh(III) denotes an upper Ru(II)-based



excited state of the binuclear complex). Let us recall that, upon single-photon MLCT excitation at 150 K, electron transfer quenching (eq 1) was inefficient (for **Ru–(ph)–Rh** and **Ru–(ph)₂–Rh**) because of the need to overcome an activation barrier and the low temperature. It seems likely that, with the excess energy available from upper excited states, the electron transfer process may become efficient under conditions of multiphotonic excitation (eq 11).

Conformational Problems. With respect to analogous systems with flexible polymethylene bridges,³⁹ the use of rigid polyphenylene bridges in these binuclear Ru(II)–Rh(III) complexes has the advantage of providing a fixed and well-known metal–metal distance. It is important to realize, however, that some conformational freedom is still present with polyphenylene bridges, in terms of rotation around formally single bonds. If the intercomponent interaction proceeds via the π system of the bridge, the tilt angle between subunits is critical,⁸¹ and this may have relevant consequences on (i) the degree of metal–metal interaction and (ii) electron transfer kinetics.

Indications of such conformational effects come especially from the results obtained with the shortest **Ru–Rh** system. For this complex, the low-energy MLCT absorption maximum (Figure 2) and low-energy MLCT emission maxima (Figure 7) point toward some delocalization of the promoted electron over the two tpy moieties of the bridge. The emission and excitation spectra obtained at 77 K (Figure 8) indicate that the extent of this delocalization is dependent on conformational freedom in the system. Actually, the emission and excitation spectra show

(78) Balzani, V.; Bolletta, F.; Scandola, F. *J. Am. Chem. Soc.* **1980**, *102*, 2152.

(79) Murtaza, Z.; Zipp, A. P.; Worl, L. A.; Graff, D.; Jones, W. E.; Bates, W. D.; Meyer, T. J. *J. Am. Chem. Soc.* **1991**, *113*, 5113.

(80) These arguments are independent of whether the energy transfer is considered to occur via a Förster or a Dexter mechanism (which is a matter of the type of electronic matrix element responsible for the process). Experimentally, any accurate evaluation of the rate constant by the usual Förster formula is prevented by the lack of appropriate data (lifetime and emission quantum yield) for the donor, Rh(III)-based excited state. The spin-forbidden nature of both virtual transitions and the poor spectral overlap between Rh(III) emission and Ru(II) absorption, however, point toward a Dexter energy transfer as the most plausible hypothesis.³⁹

(81) Helms, A.; Heiler, D.; McLendon, G. *J. Am. Chem. Soc.* **1991**, *113*, 4325; **1992**, *114*, 6227.

the simultaneous presence of species absorbing and emitting at short wavelengths (comparable to a mononuclear **Ru** model) and of others absorbing and emitting at longer wavelengths. It seems reasonable to identify such species as rotational conformers, frozen in the rigid glass, with those where the two tpy moieties of the bridge are more coplanar, being responsible for the red-shifted absorption and emission. The same behavior is exhibited by the **Ru-Ru** binuclear model complex at 77 K.

It is difficult to state in general terms whether such conformational effects are maintained or disappear in fluid solution at 150 K. For the **Ru-Ru** model, where emission/excitation spectra of the type in Figure 8 can still be measured, the wavelength effects disappear, suggesting fast equilibration between the rotational isomers. For **Ru-Rh**, on the other hand, accurate emission/excitation experiments are precluded by the strong quenching observed. The fact, however, that the residual emission exhibits a long (practically unquenched) lifetime could be an indication of the presence of a small fraction of a (highly twisted) rotational isomer with poorer electronic factors for electron transfer quenching.

It should be finally noted that for the longer **Ru-(ph)-Rh** and **Ru-(ph)₂-Rh** systems any conformational effect would be very difficult to probe experimentally. In fact, these complexes are spectroscopically almost indistinguishable from the mononuclear **Ru** model and do not undergo electron transfer quenching of the Ru(II)-based MLCT state under any condition.

Conclusions

Despite the structural suitability of this series of Ru(II)-Rh(III) dyads, the distance dependence of intercomponent electron transfer from excited Ru(II) to Rh(III) through rigid polyphen-

ylene spacers could not be experimentally probed. Due to the properties of the Ru-terpyridine chromophore, in fact, low temperatures are needed to reach excited-state lifetimes suitable for intercomponent quenching. Lowering the temperature, however, is also expected to slow considerably the electron transfer processes from excited Ru(II) to Rh(III) (which belong to the slightly exergonic, thermally activated kinetic regime). In practice, it has been impossible to find a temperature range where electron transfer quenching occurs for all members of the series. Actually, electron transfer quenching has only been observed at 150 K for the shortest member of the series, **Ru-Rh**. Under these conditions, electron transfer is inefficient in **Ru-(ph)-Rh** and **Ru-(ph)₂-Rh** because of the poorer electronic properties and larger reorganizational energies of these systems.

Interesting results of this work include the following: (i) energy transfer from excited Rh(III) to Ru(II) is efficient for all complexes at both 77 and 150 K; (ii) electron transfer quenching, which for **Ru-(ph)-Rh** and **Ru-(ph)₂-Rh** does not occur appreciably upon single-photon excitation, can be efficient following multiphotonic excitation to higher excited states; (iii) rotational isomers of **Ru-Rh**, frozen at 77 K, have spectroscopic properties suggesting varying degrees of electronic delocalization between the two moieties of the bridging ligand.

Acknowledgment. We thank Mr. O. Zerlotin for technical assistance. This work was performed with financial support from the MURST and CNR (Italy) and from the CNRS (France). A NATO grant (No. 931036, Supramolecular Chemistry) is also gratefully acknowledged.

IC950745J